Supporting Information for "Transient evolution of polar amplification under different CO_2 ramping rates"

Camille Hankel[1,2]and David B. Bonan[1,2]

[1]Department of Atmospheric and Climate Science, University of Washington, WA, USA

[2]Cooperative Institute for Climate, Ocean, and Ecosystem Studies, University of Washington, WA, USA

Contents of this file

1. Figures S1 to S15

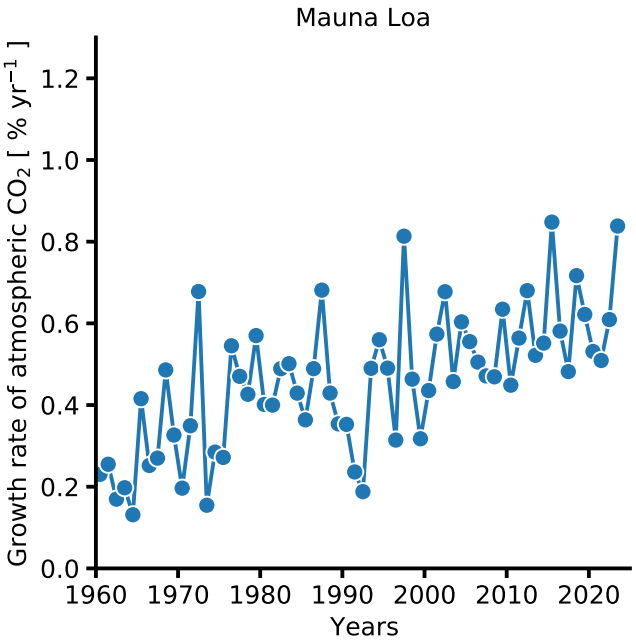

Figure S1. Annual-mean percentage increase in atmospheric CO_2 concentration for each year from 1959 to 2024, calculated based on measurements from the Mauna Loa Observatory, accessed from: `gml.noaa.gov/ccgg/trends/`.

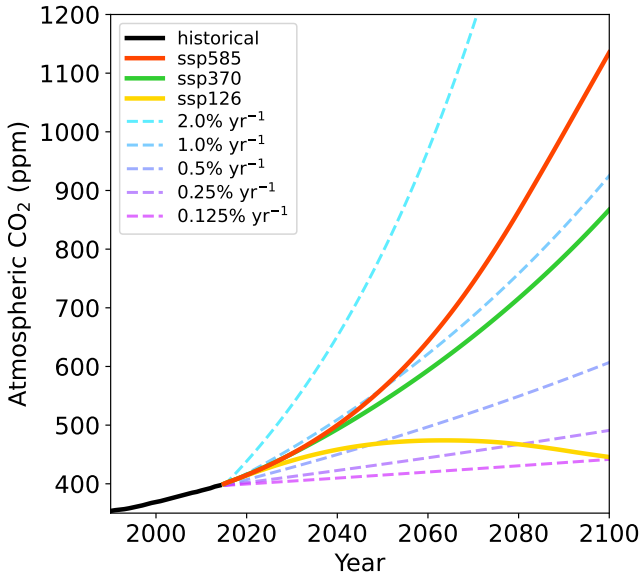

Figure S2. Annual-mean atmospheric CO_2 concentrations for three future Shared Socioeconomic Pathways (SSPs) from the CMIP6 protocol (solid lines, Meinshausen et al., 2011), and example timeseries of fixed rates of CO_2 increase (dashed lines) starting from the observed CO_2 concentration in 2014 from which the different SSP scenarios branch (397.12 ppm). The maximum yearly percentage increases in CO_2 concentrations for the three future scenarios are: 1.5% yr^{-1} (SSP585), 1.0% yr^{-1} (SSP370), and 0.8% yr^{-1} (SSP126).

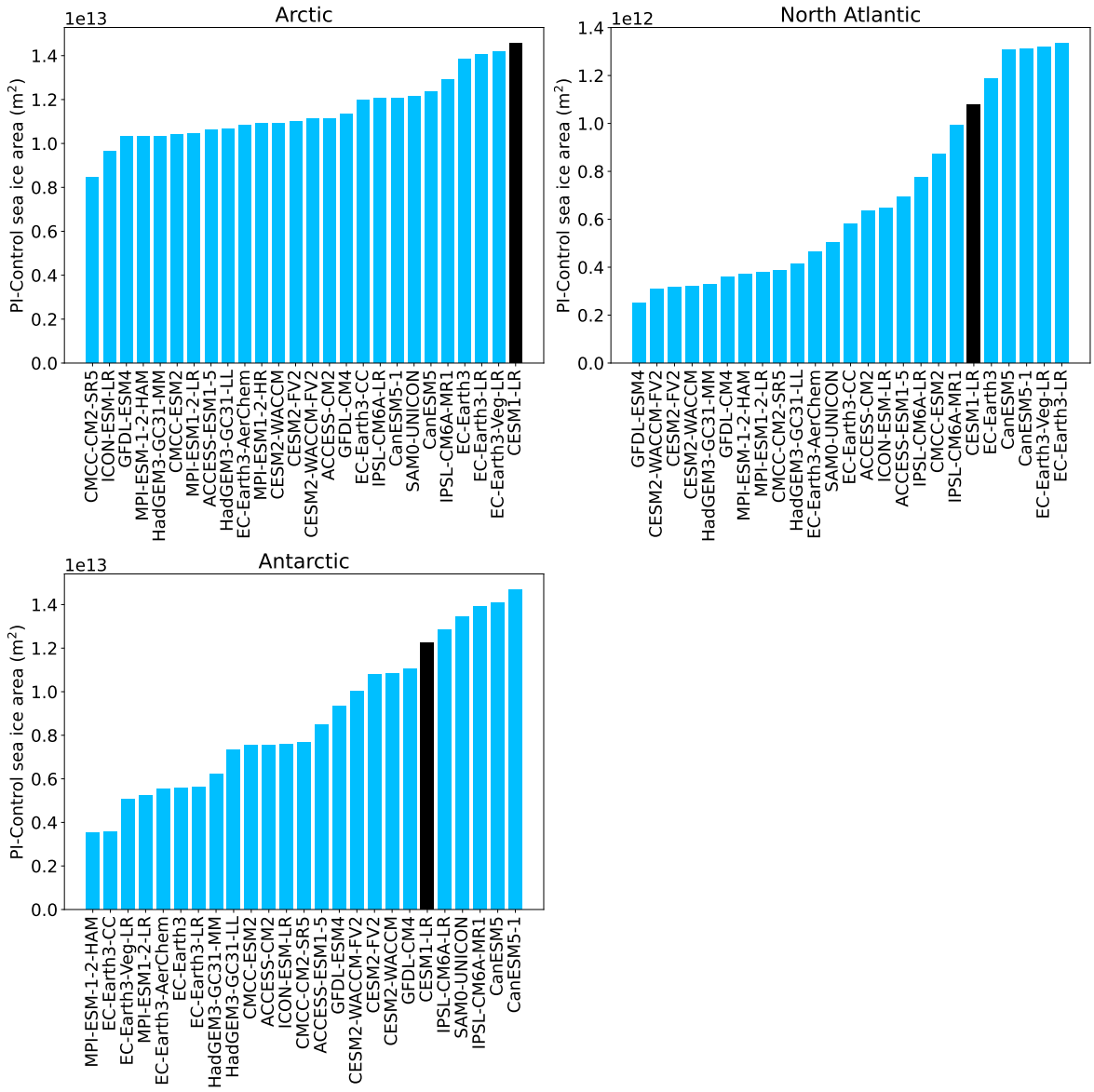

Figure S3. Mean state sea ice area for different regions in the low-resolution version of CESM1 used in this study (black bar) compared to other climate models used in CMIP6. All values are calculated as the average over the final 30 years of the preindustrial control run, and the North Atlantic region is defined as 40–65°N in the Atlantic sector. Data for CMIP6 models were accessed via the Earth System Grid Federation (https://aims2.llnl.gov/search).

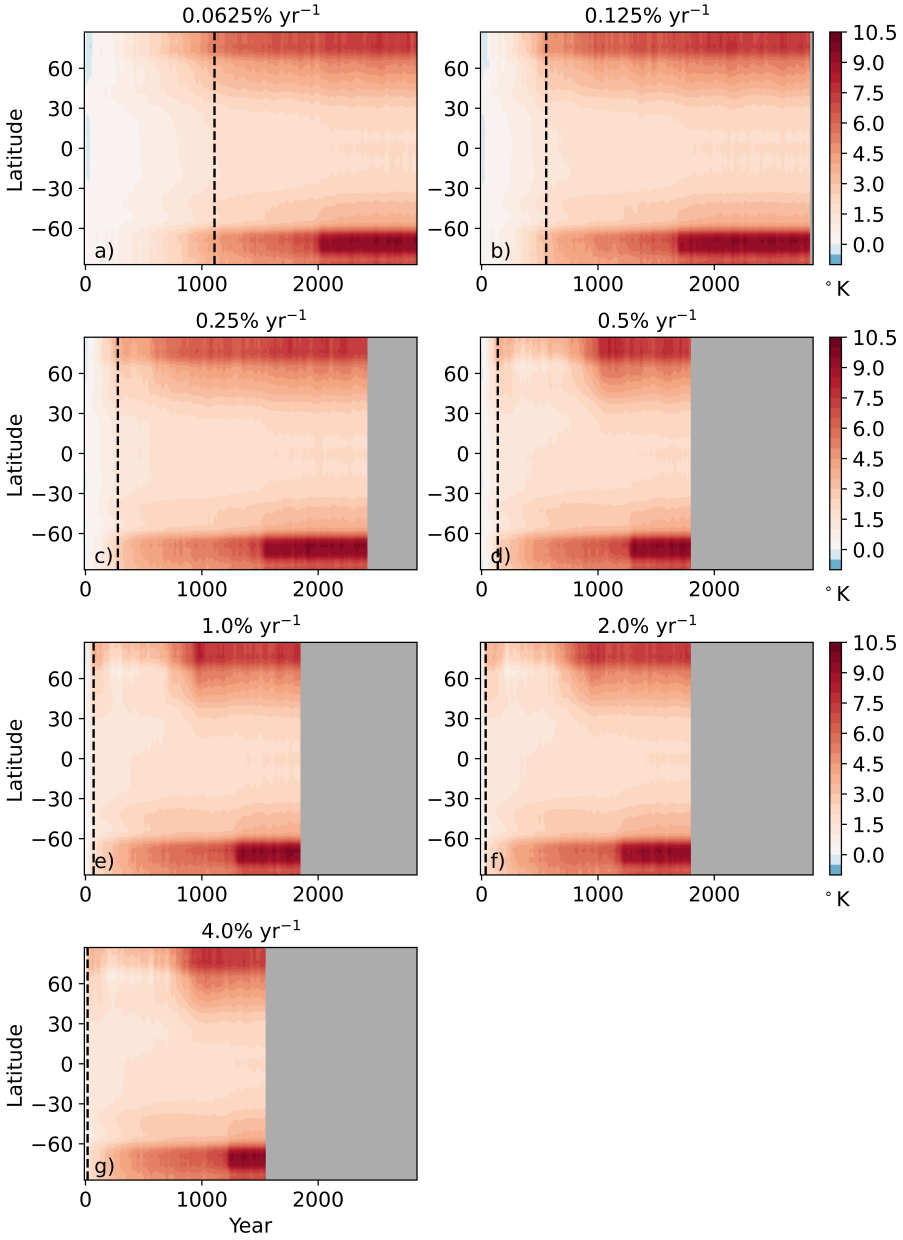

Figure S4. Anomalies in zonal- and annual-mean surface temperatures relative to the preindustrial control simulation for each ramping experiment, as indicated in the panel titles. The experiments have different simulation lengths but share the same x-axis; grayed-out regions indicate where a simulation ended. The vertical dashed black line marks the year at which $2\times CO_2$ is reached, after which atmospheric CO_2 concentrations are held fixed. A 30-year linear filter has been applied to all timeseries.

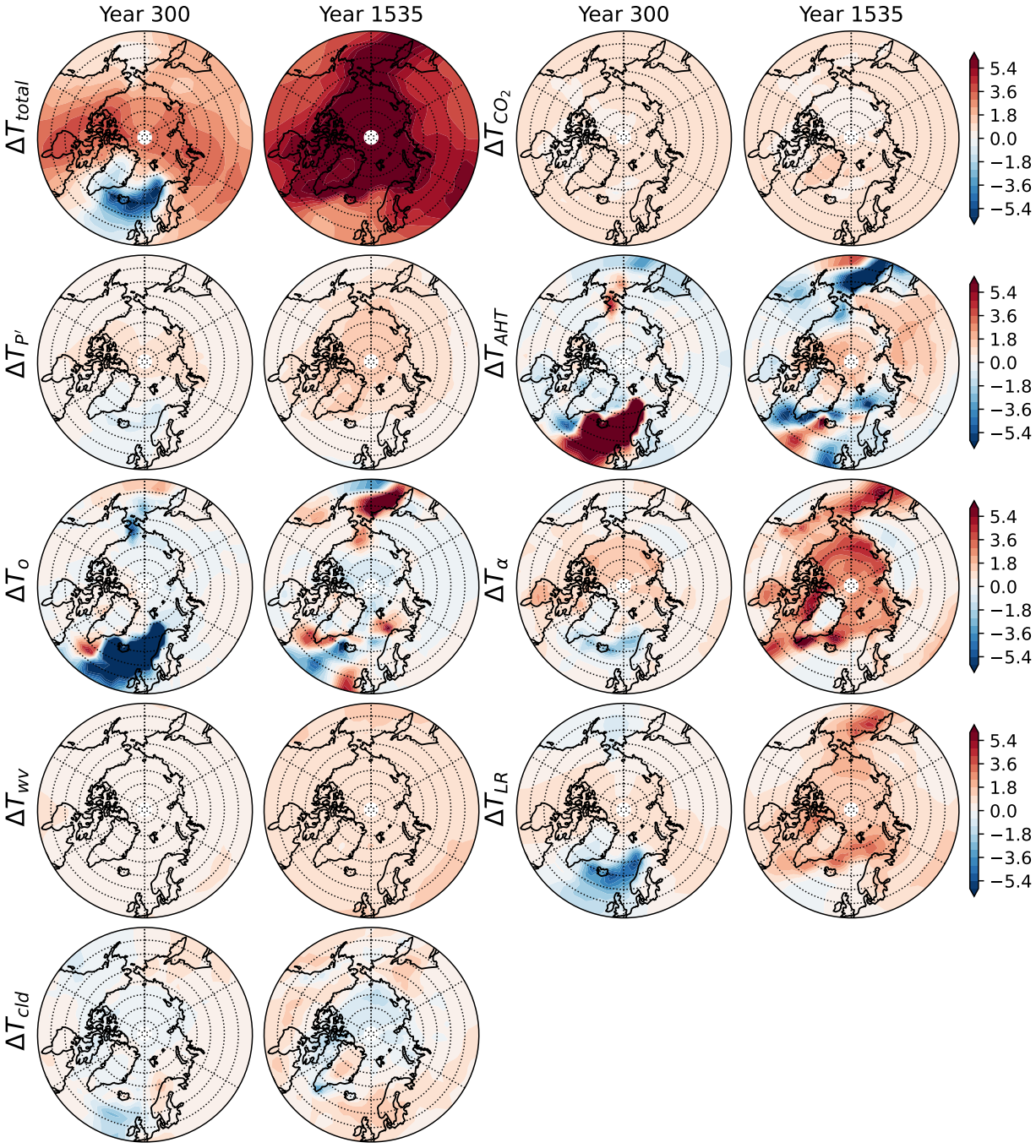

Figure S5. Spatial maps of the contributions of different mechanisms to surface temperature changes in the Arctic for the experiment with the most rapid rate of CO_2 increase (4% year^{-1}) calculated as 30-year averages centered on the years indicated in the titles.

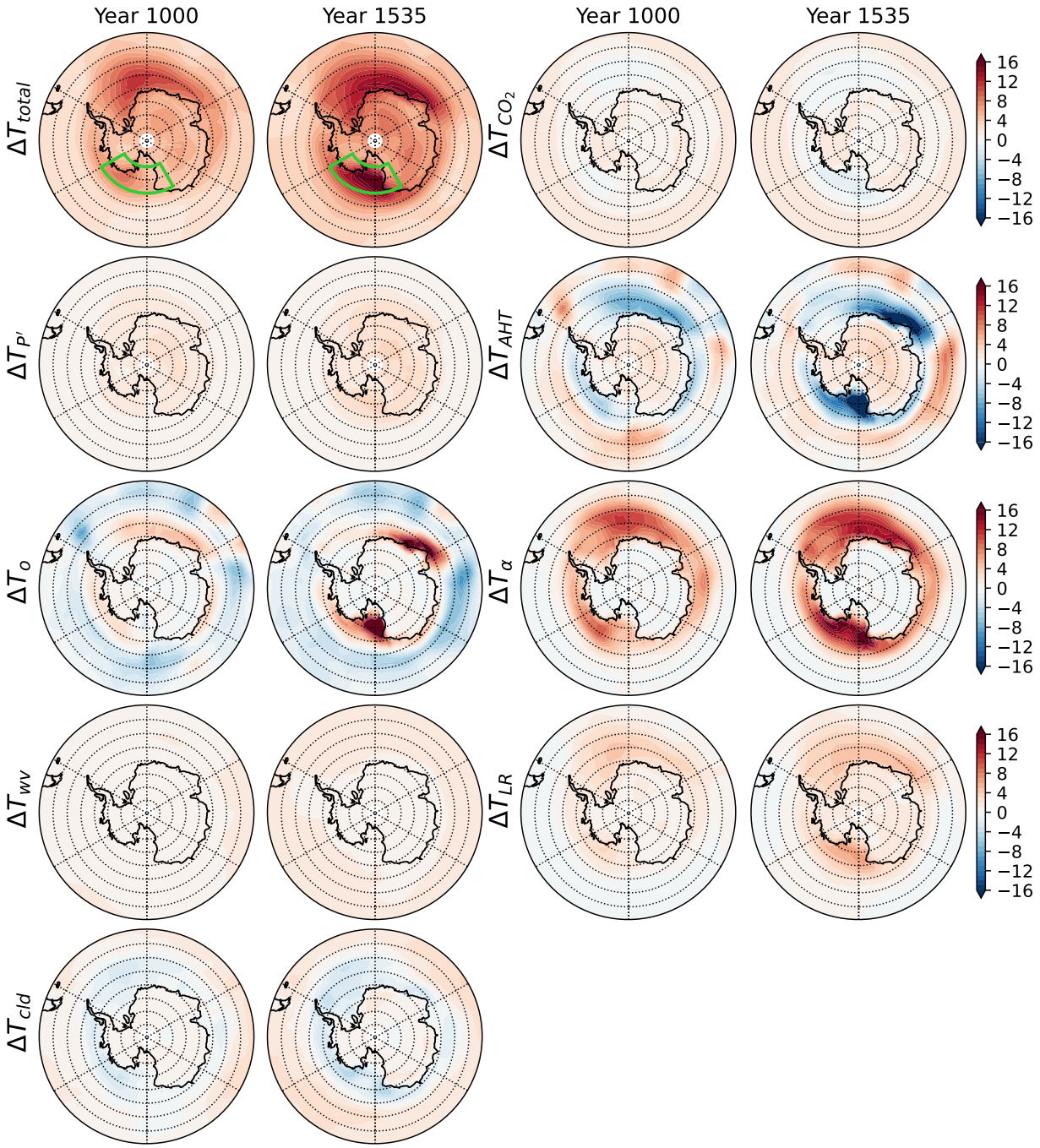

Figure S6. Same as Figure S5, but for the Antarctic region, and for the times indicated in the titles, between which the abrupt increase in the Antarctic amplification factor occurs. The green sector highlights the region of most abrupt warming between the two time periods (the Ross Sea), which is further analyzed in Figure S10.

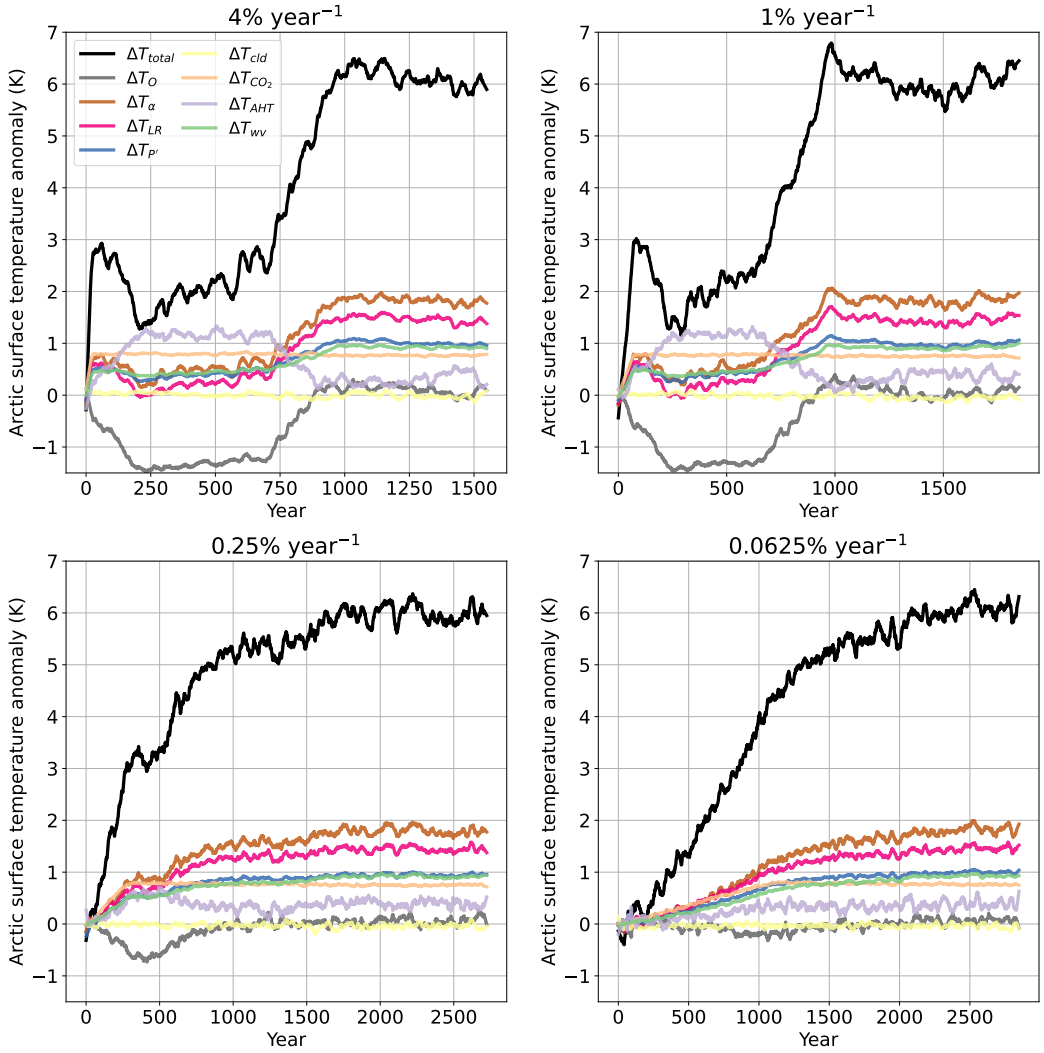

Figure S7. Timeseries of Arctic surface temperature change and all the feedback/forcing processes that contribute to it for the four ramping experiments shown in main text Figure 2, as indicated in the titles. A 30-year linear filter has been applied to smooth all timeseries.

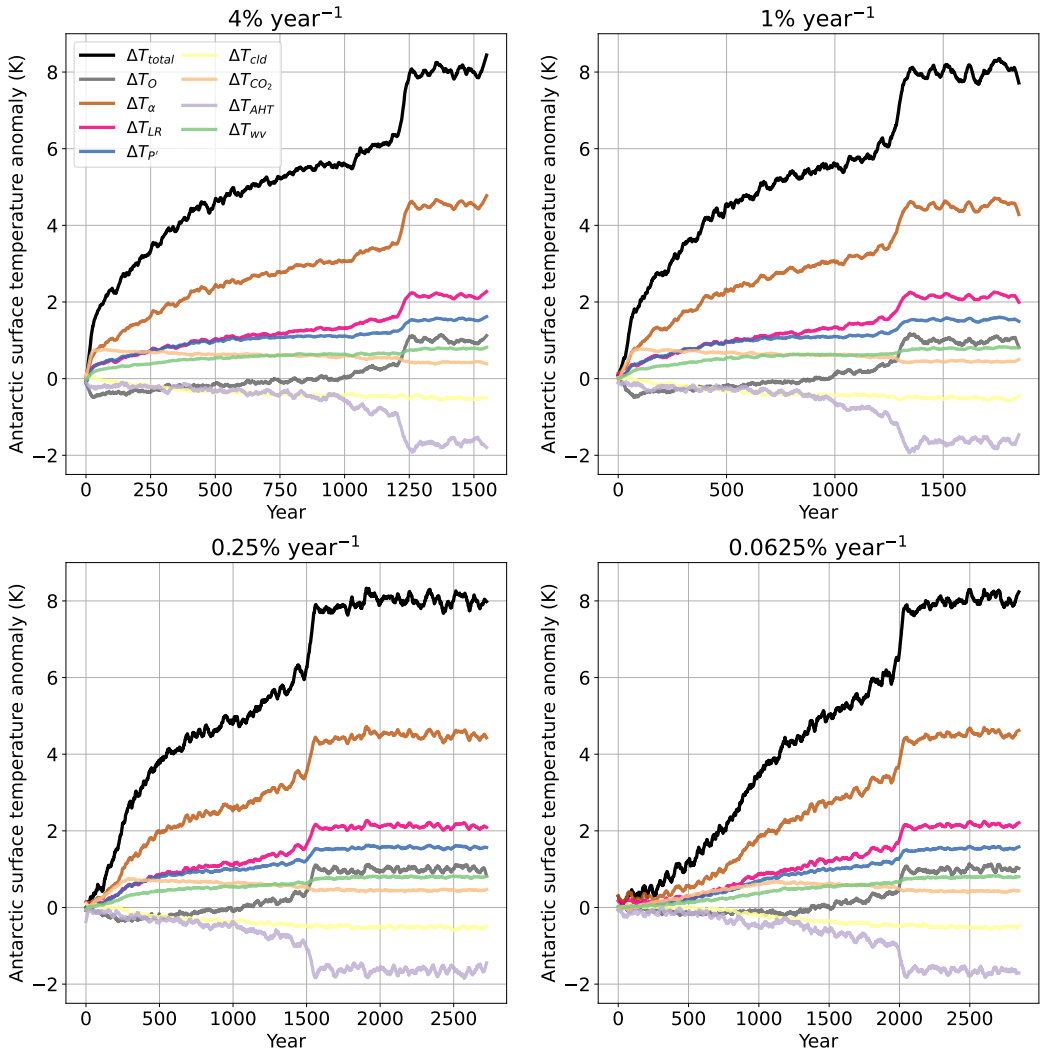

Figure S8. Same as Figure S7, but for the Antarctic.

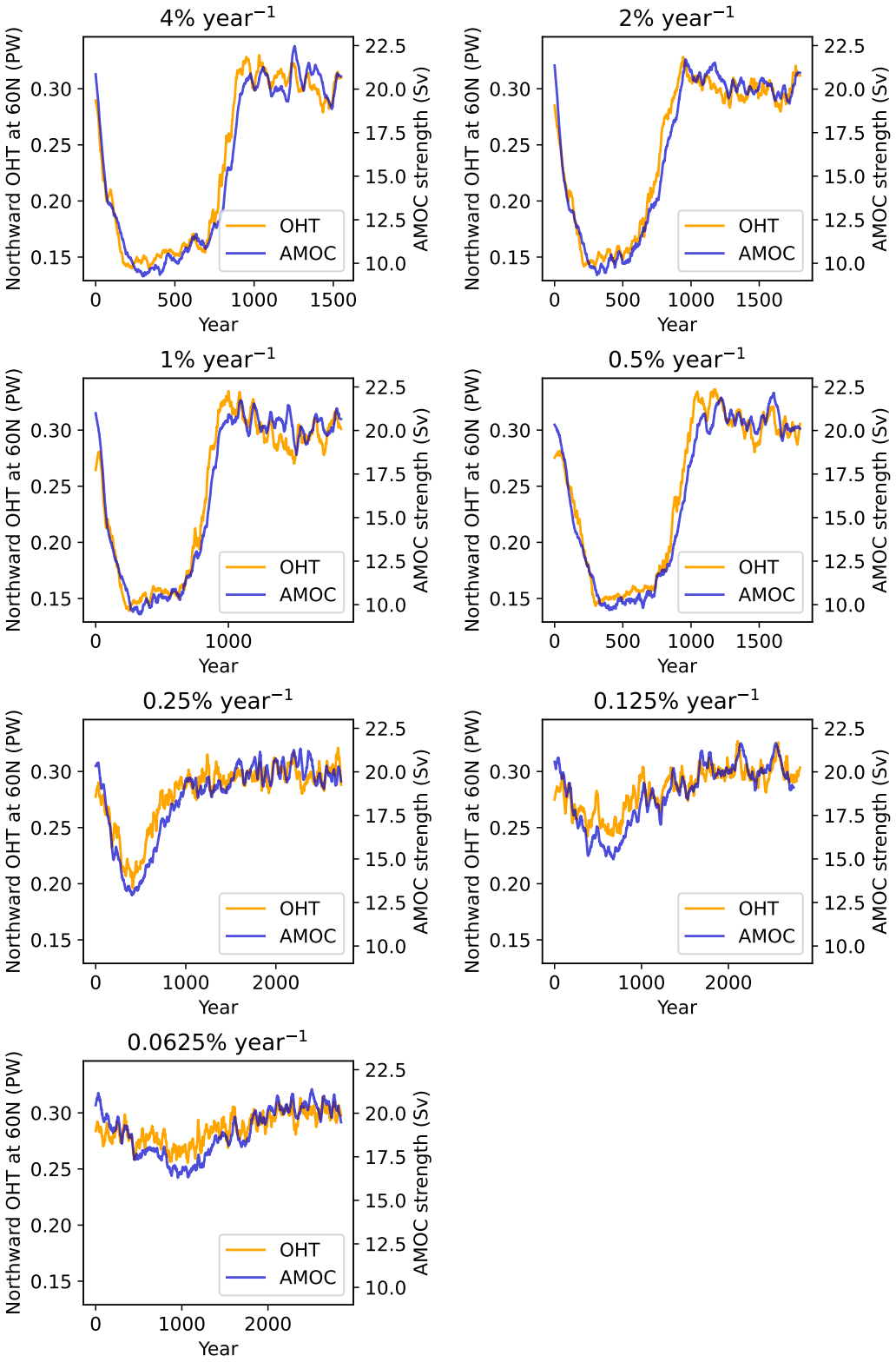

Figure S9. Northward ocean heat transport across 60°N in the Atlantic (yellow, left y-axis), and AMOC strength (blue, right y-axis) for all seven CO_2 ramping experiments. AMOC strength is defined as the maximum streamfunction value in the Atlantic basin between the equator and 65°N and below 250 m, evaluated on a monthly timescale and then averaged into an annual mean. All timeseries have been smoothed with a 30-year linear filter.

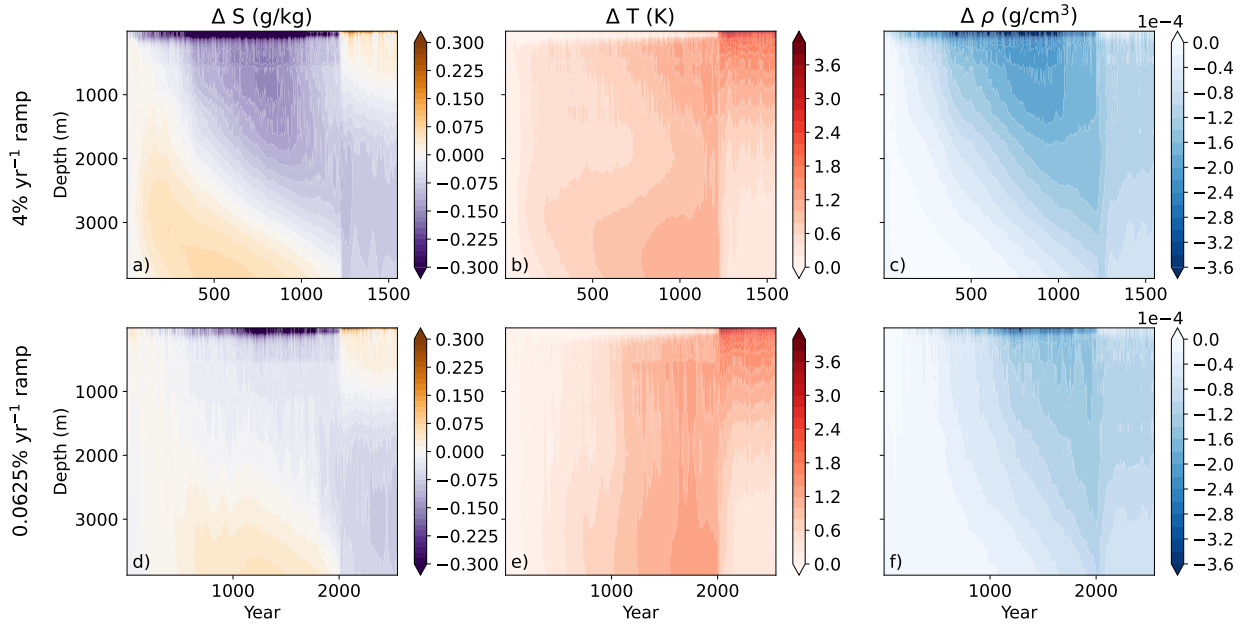

Figure S10. Anomalies of salinity (left), temperature (center), and potential density (right) with respect to the preindustrial period averaged over the Southern Ocean Ross Sea sector (highlighted in Figure S6 above). The upper row shows the most rapid CO_2 ramping experiment (4% year^{-1} increase) and the lower row shows the most gradual CO_2 ramping experiment (0.0625% year^{-1}).

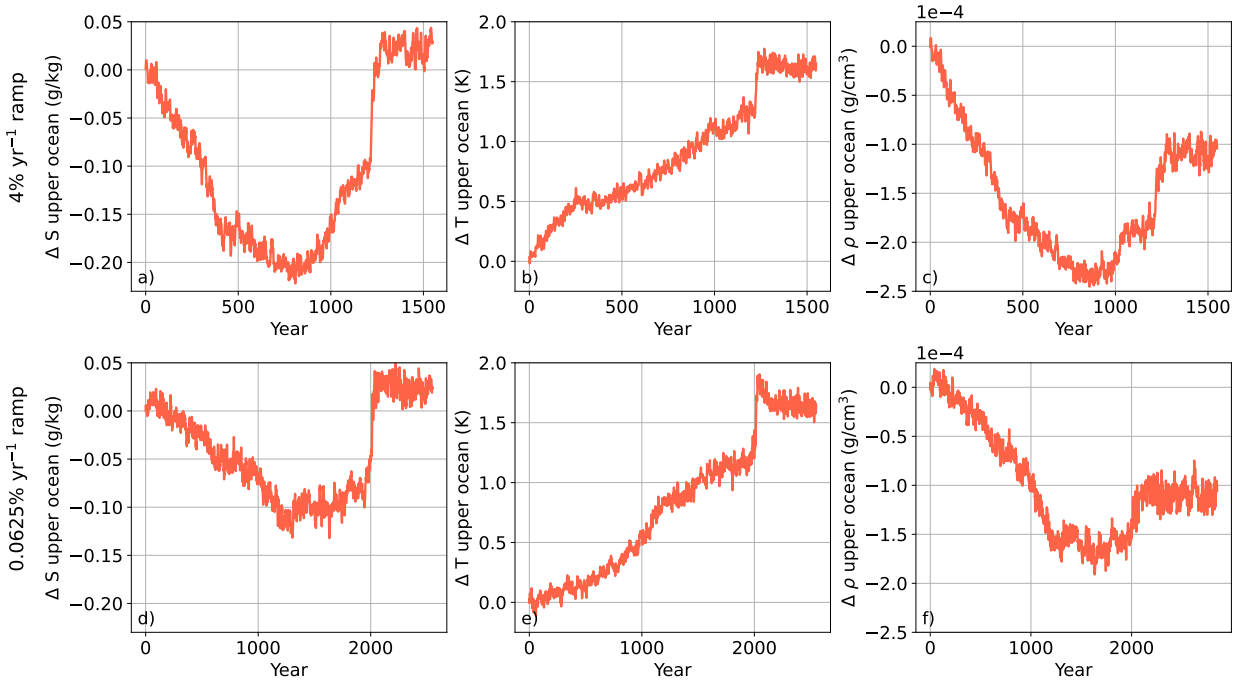

Figure S11. Average of the anomalies shown in Figure S10 over the upper 1000 m of the ocean, illustrating how the overall freshening trend switches to a gradual salinification for the several centuries preceding the convective event.

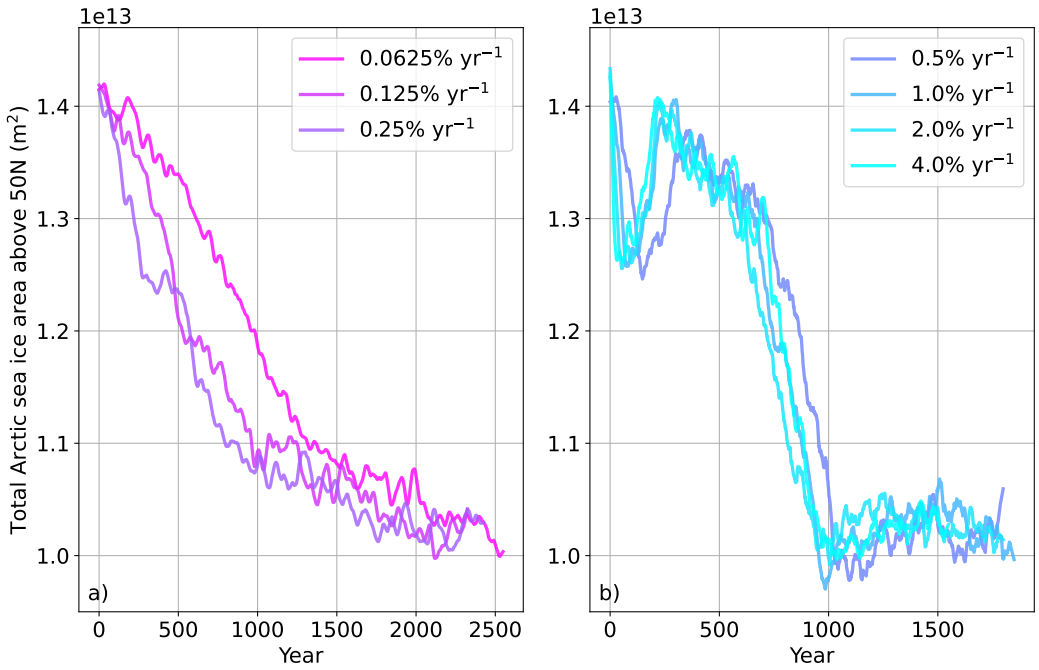

Figure S12. Total Arctic sea ice area for all CO_2 ramping experiments with a 30-year linear filter applied, separated into those experiments that did not show a transient disappearance of Arctic amplification (slower ramping rates, panel a) and those that did (faster ramping rates, panel b). Given that our forcing-feedback analysis demonstrates that reductions in northward ocean heat transport are a primary driver of suppressed Arctic amplification, we might expect a continuum of levels of suppressed Arctic amplification across the CO_2 ramping experiments that mirrors the range of levels of northward OHT reduction (Figure S9). Instead, Figure 1 in the main text reveals that the CO_2 ramping experiments fall more-or-less into two discrete groups: those whose Arctic amplification factor drops to zero (rate of CO_2 increase $\geq$ 0.5% yr^{-1}) and those that show a smooth increase in the Arctic amplification factor over time. We suggest that this may be related to the bifurcated response of Arctic sea ice to the varying rates of CO_2 increase depicted here, with the faster ramping experiments exhibiting a period of sea ice re-growth that can further suppress Arctic amplification via surface albedo and lapse-rate feedbacks.

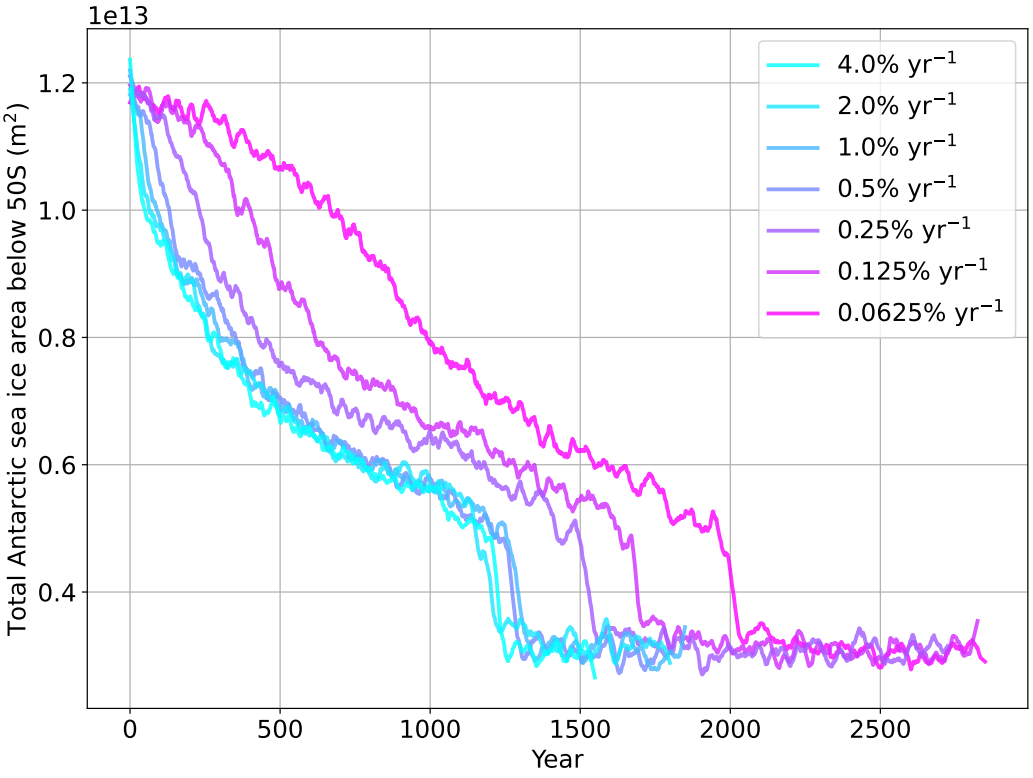

Figure S13. Total Antarctic sea ice area for all CO_2 ramping experiments, with a 30-year linear filter applied. The abrupt loss of sea ice in these timeseries is concurrent with the abrupt increase in the Antarctic amplification factor and the Ross sea convective event shown in Figure S10.

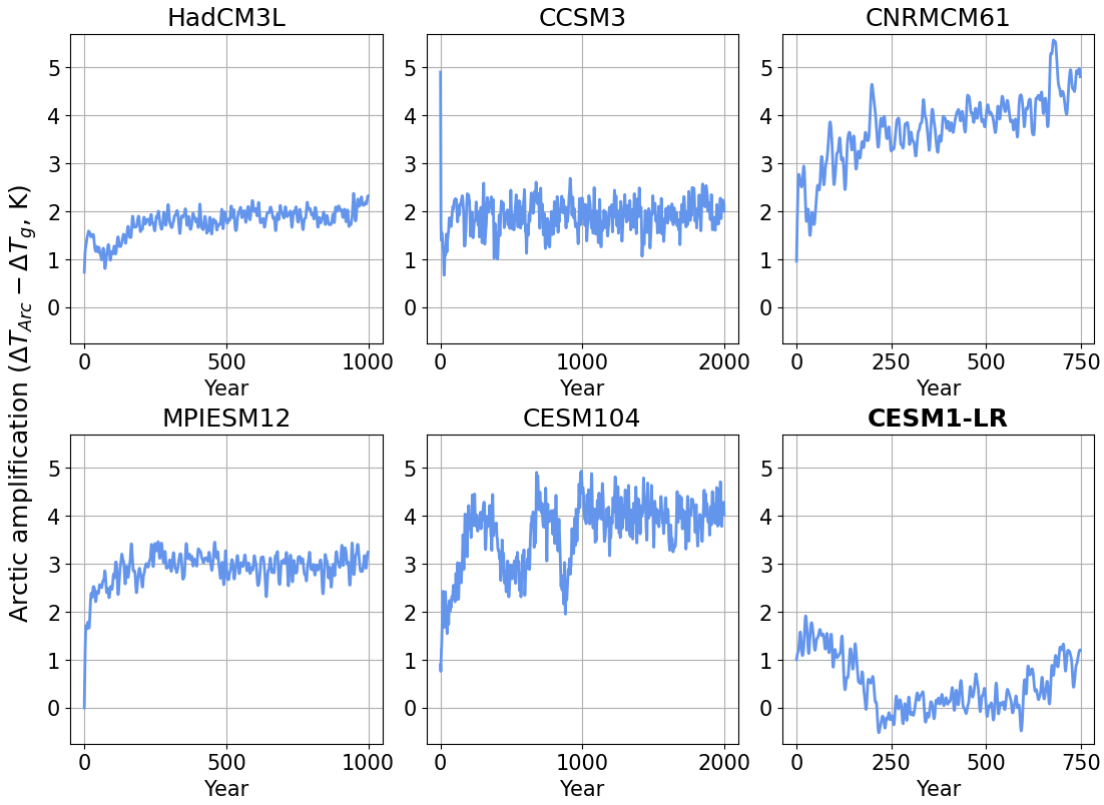

Figure S14. Arctic amplification factor for five of the models that submitted output from an instantaneous CO_2 doubling experiment to LongRunMIP, and for our model (lower right, bold), also run with an instantaneous doubling of CO_2. A 10-year Butterworth filter has been applied to all timeseries as this retains the important signals at the beginning of the timeseries that would otherwise be suppressed using the linear smoothing technique applied in the main text.

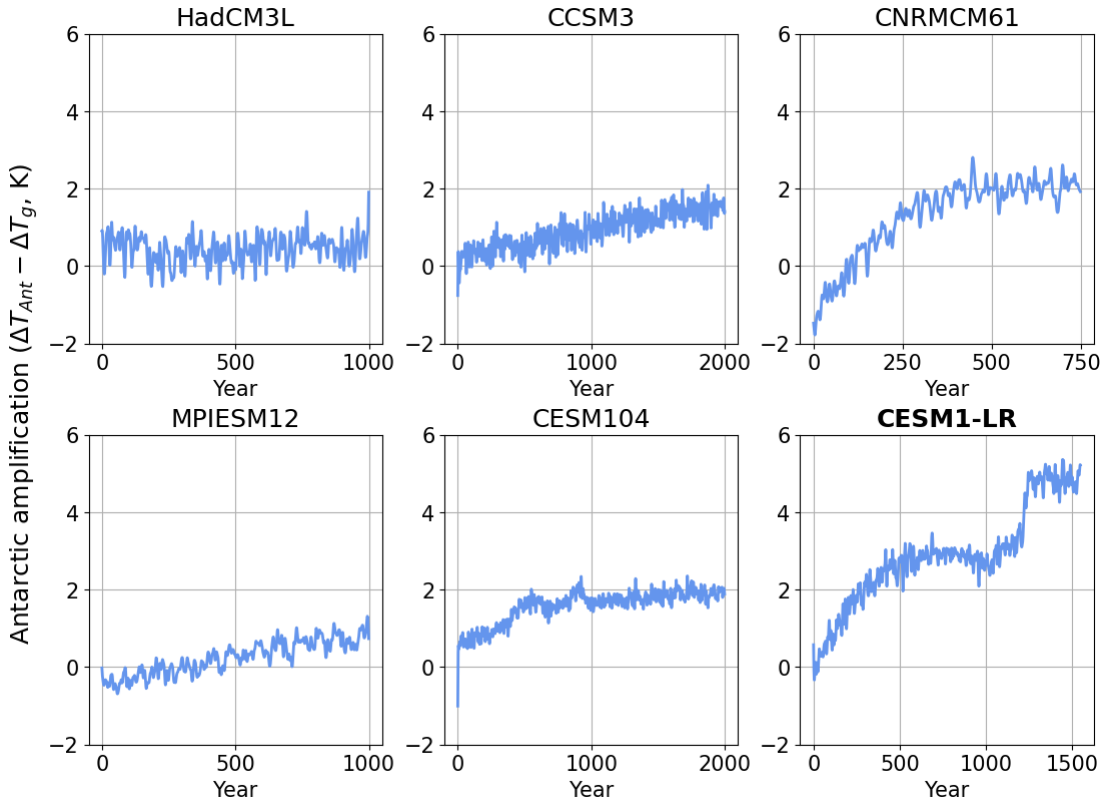

Figure S15. Same as S14, but for the Antarctic, and showing the 4% year^{-1} CO_2 ramping experiment for our model because we only run the instantaneous doubling experiment for 750 years, and thus, it does not show the abrupt jump in the amplification factor.